N. Triantafyllidis
Department of Aerospace Engineering,
University of Michigan,
Ann Arbor, Mich. 48109

R. Abeyaratne
College of Engineering,
Michigan State University,
East Lansing, Mich. 48824
Assoc. Mem. ASME

Instabilities of a Finitely Deformed Fiber-Reinforced Elastic Material

The instabilities of a finitely deformed Blatz-Ko material reinforced with fibers in a single direction (an anisotropic, nonlinearly elastic material) are examined. The loading is one of plane strain uniaxial stress with the load axis being inclined with respect to the fiber direction. In general one finds a critical applied stress (or stretch) at which surface instabilities of the body occur. This is then followed by a shear band-type instability. For a certain range of fiber orientations these instabilites appear a maximum stress level has been reached. It has also been found that when the fiber direction approaches the loading axis, the material is stabilized in tension but destabilized in compression.

1 Introduction

The mechanical properties of a ductile solid play an important role in determining its failure mechanism at high strain levels. Failure modes of particular interest are those due to a loss of stability, which can either be of a local or a global character. A local (or material) instability refers to one that occurs at a point in the body once a certain critical state of stress or strain has been reached at that point, irrespective of the conditions at the boundary. Such an instability is often associated with a shear band-type failure mode and occurs when the governing displacement equations of equilibrium lose ellipticity. On the other hand, a global (or geometric) instability is associated with a buckling type of failure that is critically dependent on the details of the boundary conditions.

A common way of strengthening certain materials, mainly elastomers, is by reinforcing them with fibers along a given direction. The present study examines the aforementioned stability properties of a fiber reinforced composite, modeled as a homogeneous, anisotropic material.

Here, attention is focused on the plane strain deformation of a hyperelastic material reinforced with a single family of fibers. More specifically, we examine the isotropic constitutive model proposed by Blatz and Ko [1] generalized in order to account for reinforcement. The choice of a Blatz-Ko material for the matrix was made because it exhibits shear band-type local instabilities at sufficiently large strain levels (Knowles and Sternberg [2]). On the other hand, in the presence of suitable reinforcement we find that *no* such local instabilities exist in the material when subjected to a state of plane strain uniaxial tension in the direction of the fibers. However, if the tensile stress is directed normal to the reinforcement, the material exhibits the same instabilities as does a Blatz-Ko material. It is apparent, therefore, that the direction of reinforcement significantly influences the stability properties of the composite.

In order to investigate the effect of the anisotropy on global stability, we study the bifurcation buckling of a plane strain, uniaxially stressed half space bounded by a traction-free surface. The buckling mode here is of the form of a surface wave exponentially decaying amplitude. For both types of instabilities we examine the dependence of the bifurcation stress (or stretch) on the fiber orientation. The effect of the relative proportion of fibers as well as the stiffness of the fibers are also considered.

The onset of surface instabilities in finitely strained orthotropic solids has been studied by Biot [3], Hill and Hutchinson [4], and others. Recently, the bifurcation of a transversely isotropic elastic material has been considered by Kurashige [5] and Arcisz [6]. These studies restrict attention to the particular (orthotropic) cases in which the applied stress is normal to and parallel to the fibers, respectively. On the other hand, material instabilities of the shear band type have been examined by Rice [7], Knowles and Sternberg [8], and others. Douglas and Jaunzemis [9] have formulated the conditions for a loss of ellipticity of a general, transversely isotropic, elastic material and analyzed the particular examples of hydrostatic pressure and simple shear. However, an investigation that studies the effect of an arbitrary direction of reinforcement on either geometric or material instabilities does not appear to have been carried out.

2 Preliminaries

Consider a body occupying the region R_0 in an undeformed configuration and let $\mathbf{X}$ denote the position vector of a typical particle. A deformation of the body is described by

$$x_i = \hat{x}_i(\mathbf{X}) \qquad (2.1)^1$$

which transforms R_0 into a region R and where $\mathbf{x}$ denotes the

Contributed by the Applied Mechanics Division for publication in the JOURNAL OF APPLIED MECHANICS.

Discussion on this paper should be addressed to the Editorial Department, ASME, United Engineering Center, 345 East 47th Street, New York, N. Y. 10017, and will be accepted until two months after final publication of the paper itself in the JOURNAL OF APPLIED MECHANICS. Manuscript received by ASME Applied Mechanics Division, May, 1982; final revision, September, 1982.

[1] All vector and tensor components are taken with respect to a fixed rectangular Cartesian frame. We use standard indicial notation with Greek and Latin subscripts having the respective ranges (1, 2) and (1, 2, 3).

which transforms R_0 into a region R and where $\mathbf{x}$ denotes the position vector of a material point in the deformed configuration. The components of the deformation gradient tensor $\mathbf{F}$ and the left and right Cauchy-Green tensors $\mathbf{B}$ and $\mathbf{C}$ are given by

$$F_{ij} = \partial \hat{x}_i / \partial X_j, \; B_{ij} = F_{ik} F_{jk}, \; C_{ij} = F_{ki} F_{kj}, \tag{2.2}$$

and in view of the invertibility of (2.1) the Jacobian of the deformation is positive, $J = \det \mathbf{F} > 0$.

If σ is the Cauchy (or true) stress tensor field accompanying the deformation at hand, the equilibrium equations, in the absence of body forces, are

$$\partial \sigma_{ij} / \partial x_j = 0, \quad \sigma_{ij} = \sigma_{ji}. \tag{2.3}$$

Suppose now that the body under consideration is homogeneous and elastic and that it possesses an elastic potential W representing the strain energy per unit undeformed volume. The components of true stress are given by

$$\sigma_{ij} = \frac{2}{J} f_{ik} F_{jl} \, \partial W / \partial C_{kl}. \tag{2.4}$$

The principal scalar invariants of the Cauchy-Green tensors $\mathbf{B}$ and $\mathbf{C}$ are

$$I_1 = C_{ii}, \quad I_2 = \frac{1}{2} (C_{ii} \, C_{jj} - C_{ij} \, C_{ij}), \quad I_3 = J^2 = \det \mathbf{C}. \tag{2.5}$$

If the material under consideration is *transversely isotropic*, with the preferential "fiber" direction in the undeformed configuration given by the (constant) unit vector A, then the elastic potential W depends on the three isotropic invariants I_1, I_2, I_3 as well as on two additional invariants I_4 and I_5 where

$$I_4 = C_{ij} \, A_i \, A_j, \quad I_5 = C_{ij} \, C_{ik} \, A_j \, A_k \tag{2.6}$$

(see Spencer [10]). It is apparent from (2.2) and (2.6) that $\sqrt{I_4}$ represents the extensional ratio $|\mathbf{FA}| / |\mathbf{A}|$ of a fiber. Consequently the deformation (2.1) carries the direction of reinforcement $\mathbf{A}$ into the direction defined locally by the unit vector $\mathbf{a}$

$$a_i = F_{ij} \, A_j / \sqrt{I_4}. \tag{2.7}$$

Under these conditions we have $W = W(\mathbf{C}, \mathbf{A}) = W(I_1, I_2, I_3, I_4, I_5)$ with the corresponding constitutive law given by (2.4)-(2.7) as

$$\sigma_{ij} = \frac{2}{J} \left\{ I_3 \frac{\partial W}{\partial I_3} \delta_{ij} + \left(\frac{\partial W}{\partial I_1} + I_1 \frac{\partial W}{\partial I_2} \right) B_{ij} - \frac{\partial W}{\partial I_2} B_{ik} \, B_{kj} + I_4 \frac{\partial W}{\partial I_4} a_i \, a_j + I_4 \frac{\partial W}{\partial I_5} (B_{jk} \, a_i \, a_k + B_{ik} \, a_j \, a_k) \right\}. \tag{2.8}$$

A special form of the elastic potential for a compressible, isotropic material was adopted by Blatz and Ko [1] on the basis of experimental data obtained by them in tests of a foam rubber. We consider here a Blatz-Ko material modified in the simplest possible manner to allow for fibers embedded in the direction $\mathbf{A}$ and take

$$W = \frac{\mu}{2} \{ I_2 I_3^{-1} + 2 I_3^{1/2} - 5 + f(I_4) \}, \quad f(I_4) = \alpha (I_4 - 1)^m. \tag{2.9}$$

The Baltz-Ko material corresponds to the choice $\alpha = 0$. Here, the infinitesimal shear modulus μ and the anisotropy parameter α are both positive (>0) and the hardening exponent m is taken to be an even, positive integar. Equations (2.8) and (2.9) yield the corresponding constitutive law

$$\sigma_{ij} = \mu \{ \delta_{ij} - \frac{1}{J} \, B_{ij}^{-1} + \frac{I_4}{J} f' \, (I_4) a_i \, a_j \}. \tag{2.10}$$[2]

[2] The Cayley-Hamilton theorem has also been used in deriving the particular form in (2.10). Kurashige [5] has previously considered such a constitutive law.

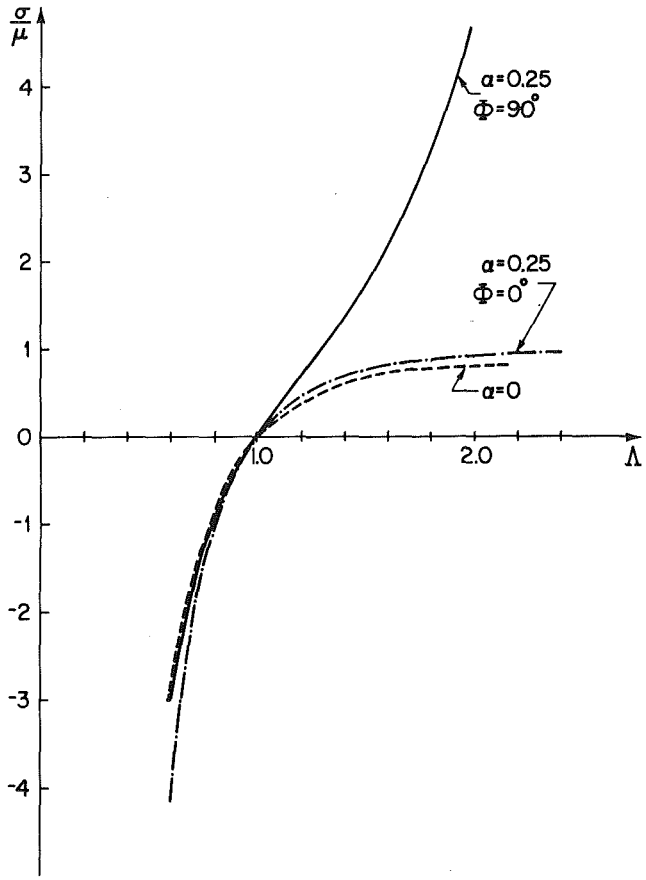

Fig. 1 Response curves in plane strain uniaxial stress. Stress versus stretch.

In order to motivate our particular choice of material, we examine a state of plane strain uniaxial stress parallel to the x_1-axis, $\sigma_{11} = \sigma$, $\sigma_{22} = 0$, $\lambda_3 = 1$. When the fibers are parallel to the direction of loading, $A_1 = 1$, $A_2 = A_3 = 0$, it can readily be shown from (2.6) and (2.10) that the applied stress σ and the transverse stretch λ_2 are related to the principal stretch $\lambda_1 = \Lambda$ by

$$\sigma / \mu = 1 - \Lambda^{-8/3} + \Lambda^{4/3} f' \, (\Lambda^2), \quad \lambda_2 = \Lambda^{-1/3}. \tag{2.11}$$

In view of the specific form of f given in (2.9) it follows that in tension $\sigma \to + \infty$ as $\Lambda \to + \infty$ and likewise in compression $\sigma \to - \infty$ as $\Lambda \to 0+$. On the other hand, if the fibers are normal to the direction of loading, $A_1 = A_3 = 0$, $A_2 = 1$, one finds that

$$\sigma / \mu = 1 - \Lambda^{-3} \lambda_2^{-1}, \quad \Lambda = \lambda_2^{-3} - \lambda_2 \, f' \, (\lambda_2^2). \tag{2.12}$$

In this case, one has $\sigma \to \mu$ as $\Lambda \to \infty$ in tension whereas in compression $\sigma \to - \infty$ as $\Lambda \to 0+$.

Figure 1 displays graphs of the stress-stretch relation σ versus Λ for the material under consideration here with $\alpha = 0.25$, $m = 2$, as well as for the isotropic Blatz-Ko material. It is clear that in tension, the fibers have a "strengthening effect" when aligned with the direction of stressing whereas they have relatively no effect when aligned in a direction normal to it. At any intermediate orientation of the fibers one expects the response to lie somewhere between these two cases.

Moreover, it may be observed in (2.12) and (2.11) that at severe extensions, $\Lambda \to + \infty$, the anisotropy term f becomes insignificant in (2.12) but that it dominates in (2.11). Thus the material behavior approaches that of a Baltz-Ko material in the former case and is quite different (much "stiffer") in the latter. As a consequence, we will find that the material loses ellipticity when the fibers are normal to the axis of loading but

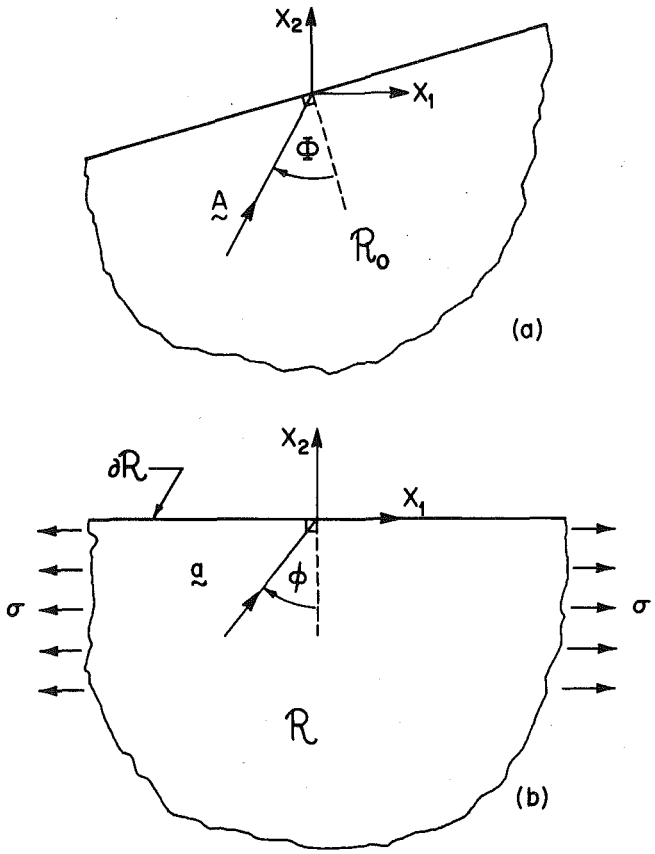

Fig. 2 Cross section of the body; (*a*) undeformed and (*b*) deformed

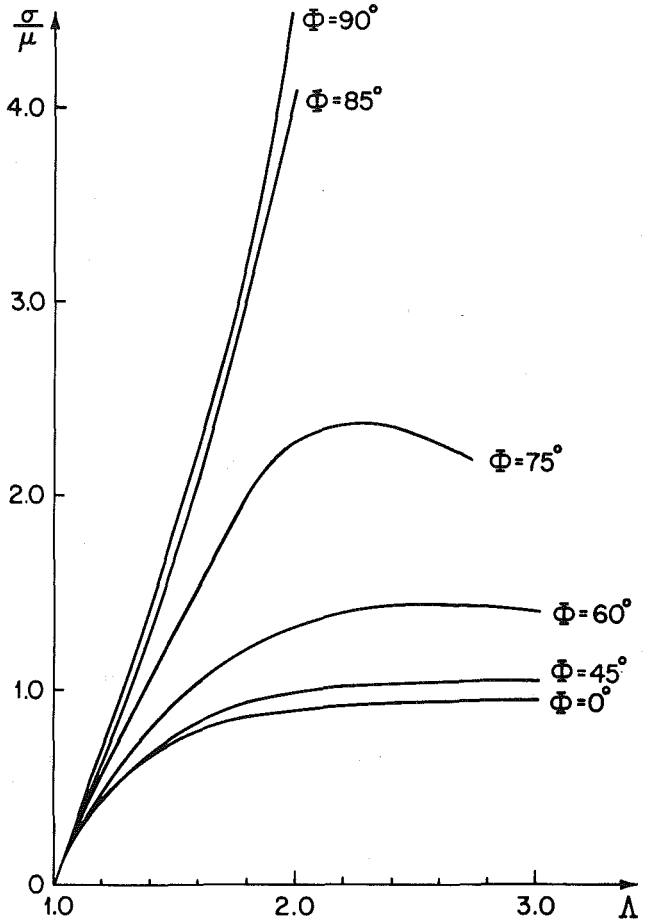

Fig. 3 Response curves in plane strain uniaxial tension. Stress versus stretch for different undeformed fiber angles Φ.

that it always remains elliptic when the fibers are parallel to it. The stability of a state of plane strain uniaxial tension may thus be expected to be highly dependent on the fiber orientation.

It is convenient to scale the stresses with respect to the infinitesimal shear modulus μ and thus we will henceforth formally set $\mu = 1$.

3 Plane Strain Uniaxial Stress

Suppose that the region occupied by the undeformed body is a half space[3] (Fig. 2(*a*)), and consider a homogeneous plane strain deformation in the plane of the fibers that leaves the boundary free of traction. We choose a rectangular Cartesian coordinate frame such that the fibers lie parallel to the $(x_1, x_2)-$plane and with the deformed half-space boundary coinciding with the $(x_1, x_3)-$plane (Fig. 2(*b*)). Then the components $F_{3\alpha}$, $F_{\alpha 3}$ of the deformation gradient tensor vanish while $F_{33} = 1$. In the case of a transversely isotropic material, this assures that the shear components $\sigma_{3\alpha}$ of the true stress tensor also vanish. Consequently the coordinate directions chosen here are principal for σ and

$$\sigma_{11} = \sigma, \sigma_{22} = 0, \quad \sigma_{ij} = 0 \ (i \neq j). \tag{3.1}$$

Since the components A_3, a_3 of the fiber directions vanish, it follows from (2.10) that $\sigma_{33} = 1 - 1/J$.

The fiber directions **A**, **a** are defined by the angles Φ, ϕ made by the fibers with a normal to the undeformed and deformed boundary, respectively (Fig. 2).

Here we view the applied stress σ and the fiber angle in the undeformed configuration Φ as being prescribed and seek to determine the deformed fiber angle ϕ and the left Cauchy-Green tensor **B**. Solving (2.10) for $\mathbf{B}^{-1}$ gives

$$B_{ij}^{-1} = J\left\{\delta_{ij} - \sigma_{ij} + \frac{I_4}{J} f'(I_4) a_i a_j\right\}. \tag{3.2}$$

Elementary manipulation[4] of equations (2.1), (2.2), (2.7) and (3.2) yields the following scalar equations:

$$\begin{aligned} J &= [I_4{}^{-1} - I_4 f'(I_4)]/(1 - \sigma \sin^2 \phi), \\ I_4 &= (1 - \sigma \cos^2 \phi) J^3/(1 + J^4 \sigma^2 \sin^2 \phi \cos^2 \phi), \\ a J^8 &+ b J^4 + c = 0, \end{aligned} \tag{3.3}$$

where

$$\begin{aligned} a &= \sigma^2(1-\sigma)^2 \sin^2 \phi \cos^4 \phi \cos^2 \Phi, \quad c = \sin^2 \phi \cos^2 \Phi, \\ b &= \{[(1-\sigma)^2 + \sigma^2 \sin^4 \phi] \cos^2 \Phi \\ &\quad - (1 - \sigma \cos^2 \phi)^2\} \cos^2 \Phi. \end{aligned} \tag{3.4}$$

The three algebraic equations in (3.3) are to be solved for J, I_4 and ϕ. Thereafter the Cauchy-Green deformation tensor **B** may be computed from (3.2) and in particular, the stretch ratio in the direction of the traction-free surface, Λ,

$$\Lambda \equiv (B_{11}{}^{-1})^{1/2} = J \cos\Phi / \sqrt{I_4} \cos\phi. \tag{3.5}$$

may be determined.

For given values of the applied stress σ and the undeformed fiber angle Φ equations (3.3) were solved numerically for the Jacobian $J(>0)$, fiber stretch ratio $\sqrt{I_4}$, and deformed fiber

[3] The results in this and the next section continue to hold true for a strip of finite dimensions.

[4] The principal steps involved consist of (*i*) computing the determinant of each side of (3.2), (*ii*) utilizing $|\mathbf{A}| = 1$ in conjunction with (2.7), and (*iii*) computing $B_{11}{}^{-1}$ from (2.7) as well as from the maping of the boundary.

angle ϕ ($0 \leq \phi \leq \pi/2$). Figure 3 displays the resulting stress-stretch response, a graph of σ versus Λ, for different values of the fiber angle Φ in the case of tension ($\sigma > 0$). Keeping in mind that the undeformed fiber angle Φ is measured from a normal to the boundary, one observes that the material becomes "stiffer" as the fiber is aligned more closely with the direction of stressing, i.e., increasing Φ. It should be noted that (except in the case $\Phi = 0$ deg, 90 deg) the stress reaches a maximum, say σ_m, at some value of stretch Λ_m as is clearly seen in the curves corresponding to $\Phi = 60$ deg, 75 deg. The value of σ_m is observed to increase with the fiber angle whereas the corresponding value of stretch Λ_m decreases.

4 Material Instabilities – Loss of Ellipticity

In this section we examine the change of the local stability properties of the composite material due to the presence of the reinforcment. After setting down the general conditions for such an instability, we examine its implications in the particular case of plane strain uniaxial stress.

The local instability criterion to be examined here is that for the onset of shear bands. Failures of this type are often observed in highly strained ductile solids. The mathematical condition corresponding to the initiation of a shear band at a given point in a body is the loss of ellipticity of the displacement equations of equilibrium at the point in question (Rice [6], Knowles and Sternberg [8]).

If $\mathbf{u}(\mathbf{x})$ denotes a further incremental displacement field from a homogeneous equilibrium state of a finitely deformed hyperelastic body, the corresponding incremental equilibrium equations linearized about this configuration are (Douglas and Jaunzamis [9])

$$L_{ijkl}\, u_{k,lj} = 0 \quad \text{on} \quad R. \tag{4.1}$$

Here a comma followed by a subscript denotes partial differentiation with respect to the corresponding x-coordinate. The incremental moduli L_{ijkl} are given by

$$L_{ijkl} = \frac{4}{J} F_{ip}\, F_{jq}\, F_{kr}\, F_{ls} \frac{\partial^2 W}{\partial C_{rs} \partial C_{pq}} + \sigma_{lj}\, \delta_{ik} \tag{4.2}$$

where $\boldsymbol{\sigma}$, $\mathbf{F}$, and J denote the Cauchy stress tensor, deformation gradient $\mathbf{F}$, and Jacobian associated with the homogeneous equilibrium state. In the case of the reinforced Blatz-Ko material (2.9) these moduli may be explicitly calculated, leading to

$$\begin{aligned} L_{ijkl} = \frac{2}{J} 3\{ & B_{ij}\, B_{kl} - \frac{1}{2}(B_{ik}\, B_{jl} + B_{il}\, B_{jk}) \\ & - I_1 B_{ij}\, \delta_{kl} + B_{kl}\, \delta_{ij}) \\ & + (B_{in}\, B_{nj} \delta_{kl} + B_{kn}\, B_{nl}\, \delta_{ij}) \\ & + (I_2 + \frac{1}{2} J^3)\delta_{ij}\, \delta_{kl} + \frac{1}{2}(I_2 - J^3)(\delta_{ik}\delta_{jl} + \delta_{il}\delta_{jk}) \\ & + I_4^2 J^2 f''(I_4) a_i a_j a_k a_l \} + \sigma_{lj}\delta_{ki}. \end{aligned} \tag{4.3}$$

The incremental equilibrium equations (4.1) are elliptic if and only if

$$\det (L_{ijkl}\, m_j\, m_l) \neq 0 \tag{4.4}$$

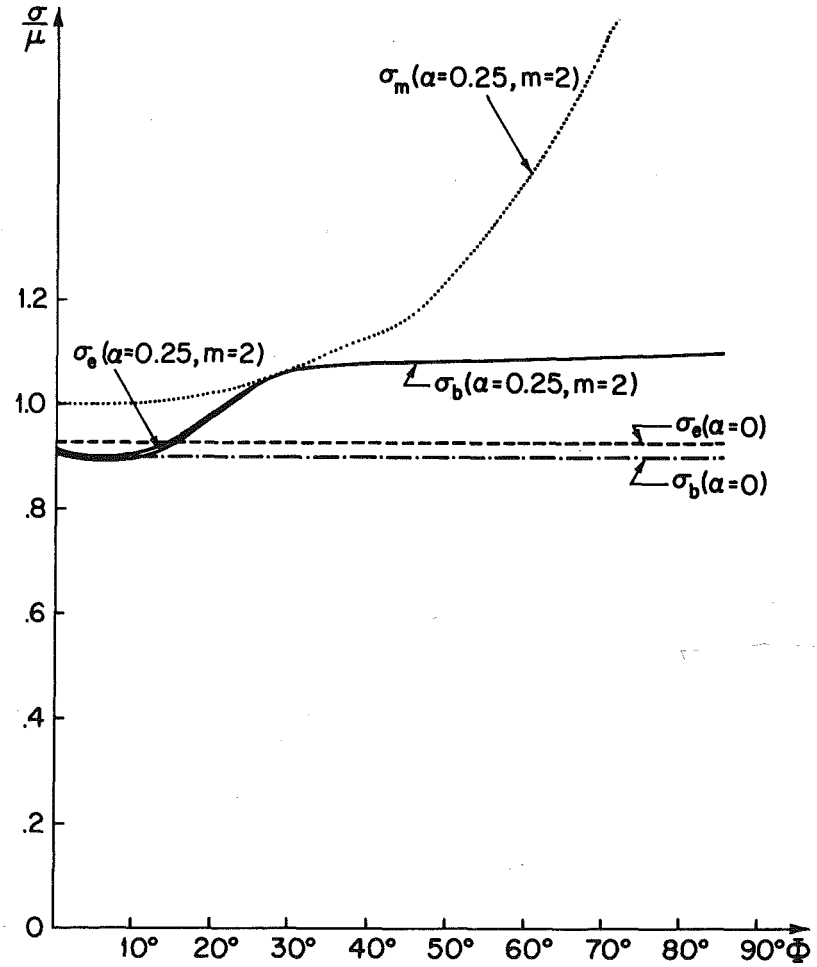

Fig. 4 Variation of the critical stresses σ_b, σ_e with fiber orientation (tension). Lises $\alpha = 0$ corresponds to unreinforced material.

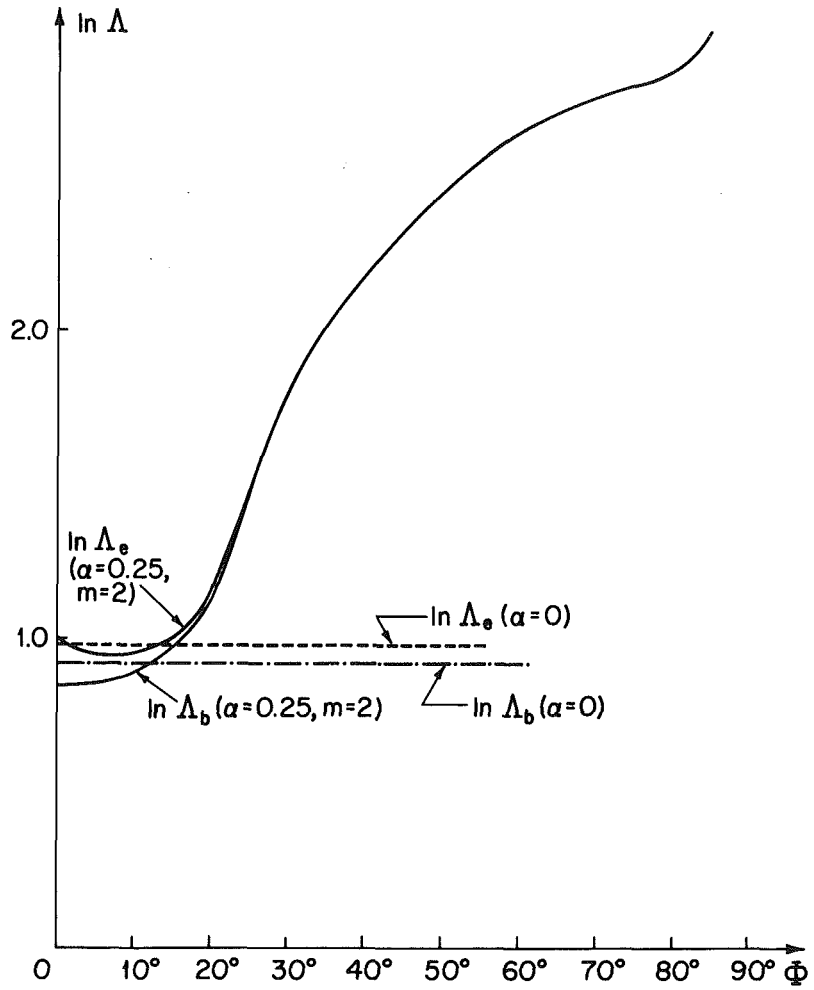

Fig. 5 Variation of the critical stretches with fiber orientaiton (tension)

for every unit vector **m**. When specialized to plane strain (4.4) yields

$$P(Z) = \det [L_{\alpha 2\beta 2} Z^2 + (L_{\alpha 1\beta 2} + L_{\alpha 2\beta 1}) Z + L_{\alpha 1\beta 1}] \neq 0 \quad (4.5)$$

for all real numbers Z ($Z = m_2/m_1$). A loss of ellipticity of the material is therefore equivalent to the presence of at least one real zero of the characteristic polynomial $P(Z)$.

In the particular case of a state of plane strain uniaxial stress the polynomial $P(Z)$ can be written explicitly by substituting the field quantities determined in Section 3 into (4.3) and (4.5). The question of a loss of ellipticity may then be addressed by studying the zeros of $P(Z)$. This was carried out numerically. For various fiber orientations Φ, we determined the stress σ (or stretch Λ) at which ellipticity fails; the results are discussed in Section 6.

In the special case when the fibers are oriented parallel to the traction-free boundary, $\Phi = \pi/2$, one finds from (2.11), (3.2), and (3.3) that

$$\begin{aligned} L_{1111} &= 3\lambda_1^{-8/3} + \lambda_1^{4/3} f'(\lambda_1^2) + 2\lambda_1^{10/3} f''(\lambda_1^2), \\ L_{2121} &= 1 + \lambda_1^{4/3} f'(\lambda_1^2), \\ L_{1212} &= L_{1221} = L_{2112} = \lambda_1^{-8/3}, \\ L_{1122} &= L_{2211} = 1, \quad L_{2222} = 3. \end{aligned} \quad (4.6)$$

where $f(\lambda_1^2) = \alpha(\lambda_1^2 - 1)^m$ and with the remaining inplane moduli being zero. It is not difficult to show that in this case the polynomial $P(Z)$ in (4.5) is now a biquadratic, and that for sufficiently large values of α, its coefficients are all positive when $\lambda_1 > 1$ (or equivalently $\sigma > 0$). Thus with suitable reinforcement, loss of ellipticity can always be prevented for tensile loading parallel to the fibers. On the other hand, one can readily show that the characteristic polynomial always has a real root, and so ellipticity is lost, in the presence of a sufficiently large compressive stress σ. This is also true, both in tension and compression, when the fibers are oriented normal to the loading direction ($\Phi = 0$).

5 Geometric Instabilities – Surface Bifurcation

Material instabilities in the form of shear localization occur at rather high strain levels. In general, and depending on the specific geometry and boundary conditions, a buckling-type global instability often precedes the onset of the more severe local instabilities mentioned in the preceding section. A simple problem that can be used to investigate the effect of reinforcement on the geometric stability of the Blatz-Ko material is the buckling of a half space under conditions of plane strain uniaxial stress. As will be subsequently see, the bifurcation mode is a surface-type mode whose amplitude decays exponentially with the distance from the free surface.

A bifurcation eigenmode $\mathbf{u}(\mathbf{x})$ is required to satisfy the incremental equilibrium equations (4.1), the traction boundary condition on the free surface (Douglas and Jaunzemis [9])

$$L_{\alpha\beta\gamma\delta} u_{\gamma,\delta} n_\beta = 0 \quad \text{on} \quad \partial R, \quad (5.1)$$

and decay condition at infinity,

$$u_\alpha \to 0, \; u_{\alpha,\beta} \to 0 \quad \text{as} \quad |\mathbf{x}| \to \infty, \quad x_2 < 0. \quad (5.2)$$

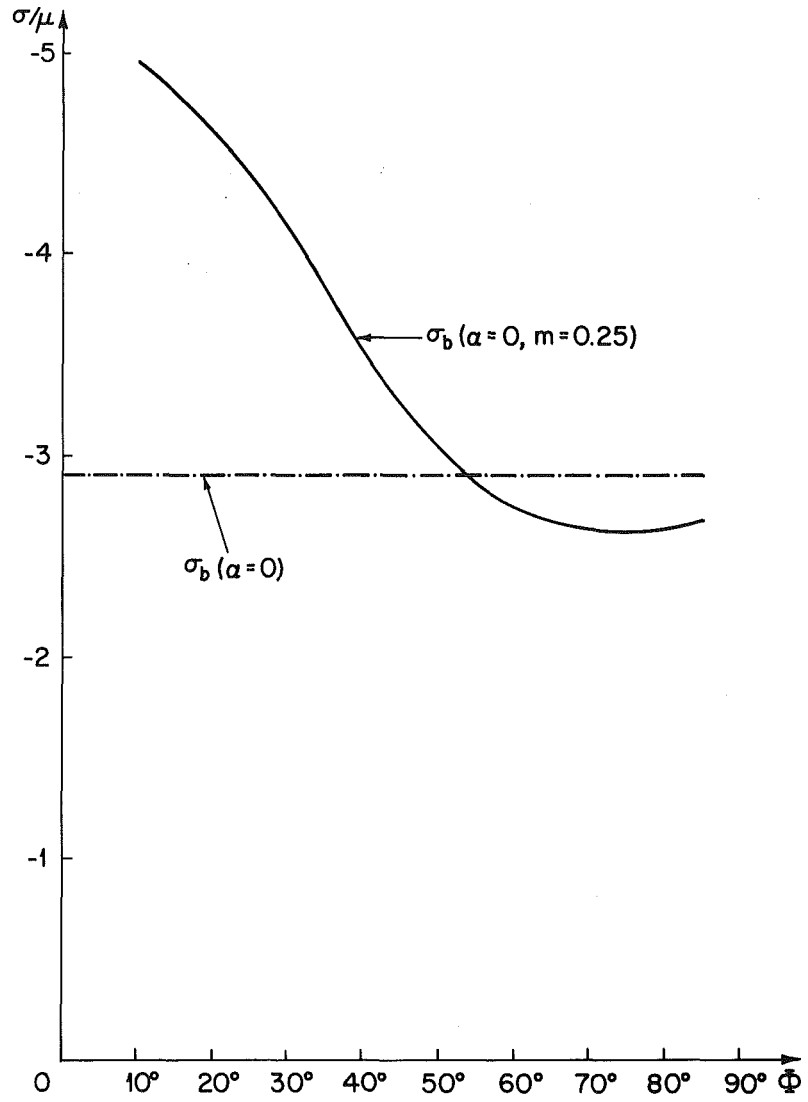

Fig. 6 Variation of the critical buckling stress σ_b with the fiber orientation (compression)

Assuming that the buckling eigenmode $\mathbf{u}(\mathbf{x})$ is twice continuously differentiable and bounded on the half space R, one can always ensure the existence of a Fourier transform $\tilde{\mathbf{u}}(\omega, x_2) = \mathfrak{F}\{\mathbf{u}(x_1, x_2) | x_1 \to \omega\}$ in the sense of distributions (Schwartz [12]). Although $\mathbf{u}$ is required to be a function in the classical sense, $\tilde{\mathbf{u}}$ in general will not be so. Consequently, the subsequent equations (5.3)–(5.8) of this section are to be interpreted in the distribution sense.

On taking the Fourier transform of the equilibrium equations (4.1) with respect to x_1 we obtain the following ordinary differential equation with respect to x_2 for $\tilde{\mathbf{u}}$

$$L_{\alpha 2\beta 2}\tilde{u}_{\beta,22} - i\omega(L_{\alpha 1\beta 2} + L_{\alpha 2\beta 1})\tilde{u}_{\beta,2} - \omega^2 L_{\alpha 1\beta 1}\tilde{u}_\beta = 0, \tag{5.3}$$

whose solution conforming to the decay condition (5.2) is

$$\tilde{u}_\alpha(\omega, x_2) = \begin{cases} \xi_1(\omega)A_\alpha^{(1)} \exp(-i\omega x_2 Z^{(1)}) + \xi_2(\omega)A_\alpha^{(2)} \exp(-i\omega x_2 Z^{(2)}) & \text{for } \omega > 0, \\ 0 & \text{for } \omega = 0, \\ \xi_1(\omega)\bar{A}_\alpha^{(1)} \exp(-i\omega x_2 \bar{Z}^{(1)}) + \xi_2(\omega)\bar{A}_\alpha^{(2)} \exp(-i\omega x_2 Z^{(2)}) & \text{for } \omega < 0. \end{cases} \tag{5.4}$$

Here $Z^{(1)}$ and $Z^{(2)}$ are the roots of the characteristic polynomial (4.5) which have positive imaginary part and a bar denotes complex conjugation. The complex (constant) unit vectors $\mathbf{A}^{(1)}$ and $\mathbf{A}^{(2)}$ satisfy

$$\{L_{\alpha 2\beta 2}(Z^{(\gamma)})^2 + (L_{\alpha 1\beta 2} + L_{\alpha 2\beta 1})Z^{(\gamma)} + L_{\alpha 1\beta 1}\} A_\beta^{(\gamma)} = 0 \quad \text{(no sum on } \gamma) \tag{5.5}$$

and ξ_1, ξ_2 are arbitrary generalized functions of ω. It should be noted that the existence of four complex roots of $P(Z)$ is ensured by the fact that we are focusing attention on the buckling modes that occur before the material loses ellipticity (and thus $P(Z)$ has no real roots).

Taking the Fourier transform of the traction-free boundary condition (5.1) gives

$$L_{\alpha 2\beta 2}\tilde{u}_{\beta,2} - i\omega L_{\alpha 2\beta 1}\tilde{u}_\beta = 0 \quad \text{for} \quad x_2 = 0, \tag{5.6}$$

since $n_1 = 0$, $n_2 = 1$. On using (5.4) in (5.6) one finds that the coefficients ξ_1, ξ_2 must necessarily satisfy

$$S_{\alpha\beta}\xi_\beta = 0 \quad \text{for} \quad \omega > 0, \quad \bar{S}_{\alpha\beta}\xi_\beta = 0 \quad \text{for} \quad \omega < 0, \tag{5.7}$$

with

$$S_{\alpha\beta} = L_{\alpha 2\gamma 2}Z^{(\beta)}A_\gamma^{(\beta)} + L_{\alpha 2\gamma 1}A_\gamma^{(\beta)} \quad \text{(no sum on } \beta). \tag{5.8}$$

Since according to (5.4) ξ_α cannot have pointwise support at

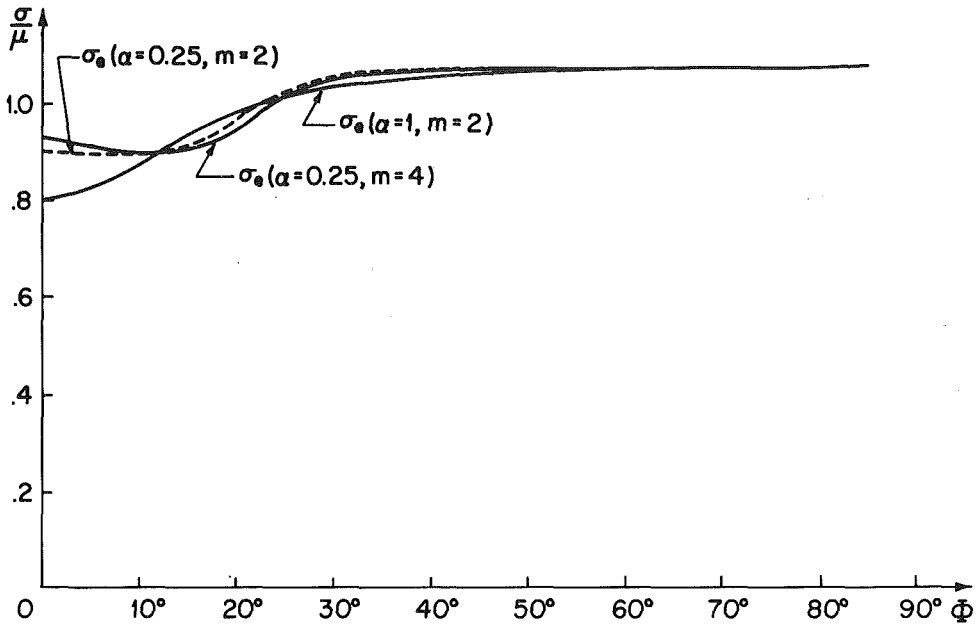

Fig. 7 Variation of the critical stress σ_e with the fiber orientation for different materials

$\omega = 0$, if a nontrivial solution (ξ_1, ξ_2) to (5.7) is to exist, it is necessary and sufficient that

$$\det S = 0, \tag{5.9}$$

which then ensures the existence of a nontrivial buckling eigenmode.

The *buckling condition* (5.9) was examined numerically for various fiber orientations Φ and the smallest value of the applied stress σ (or stretch Λ) for which (5.9) holds was determined. The results are described in Section 6.

One can easily deduce from (5.3) that $\mathbf{u}(x_1, x_2)$ decays exponentially with the depth x_2 from the free surface. The analysis does not, however, determine the x_1-dependence of the eigenmode. This is, of course, to be expected in view of the absence of any characteristic length in the problem.

Finally we note that bifurcation problems of this type have been previously considered by Biot [3], Hutchinson and Tvergaad [11], and others for orthotropic materials. These studies preassume the form of the bifurcation eigenmode and thus, at least in principle, lead to conditions that are necessary for buckling in the prescribed eigenmode only.

6 Results and Discussion

The numerical results reported here for the onset of a surface bifurcation and the loss of ellipticity of the reinforced Blatz-Ko material were based on a straightforward numerical implementation of the analysis presented in Sections 4 and 5. Of main interest in these calculations has been the dependence of the bifurcation and loss of ellipticity stresses σ_b, σ_e, (and the corresponding surface stretch ratios Λ_b, Λ_e), on the fiber angle Φ. The influence of the "density of reinforcement" which was assumed to be represented by the parameter α in the constitutive model (2.9) as well as that of the "fiber stiffness" characterized by the exponent m in the aforementioned equation was also examined.

For purposes of references we note that the unreinforced (isotropic) Blatz-Ko material loses ellipticity at $\sigma_e/\mu \simeq -13.17$, ($\Lambda_e \simeq 0.37$) in compression, [2]. Similarly a surface-type bifurcation first occurs at $\sigma_b/\mu \simeq 0.915$ ($\Lambda_b \simeq 2.52$) in tension and at $\sigma_b/\mu \simeq -2.9$ ($\Lambda_b \simeq 0.6$) in compression, [5].

In Fig. 4 we have plotted σ_b and σ_e versus Φ for plane strain tension ($\sigma > 0$) in the case of a material with $\alpha = 0.25$ and $m = 2$. Note that the value of σ_e is very close to that of σ_b (with $\sigma_e \geq \sigma_b$ for Φ less than $\simeq 27$ deg and $\sigma_b \geq \sigma_e$ for Φ greater than $\simeq 27$ deg. For fiber angles Φ exceeding $\simeq 27$ deg it is almost impossible to distinguish between the stress levels corresponding to bifurcation and loss of elliptiticy. For sufficiently small values of Φ the fibers in fact *weaken* the material with respect to its stability, with the instabilities occuring at stress levels that are less than the corresponding values for the isotropic case. Thereafter, the critical stresses σ_b, σ_e increase continuously with Φ. The relatively slow increase in σ_b and σe with respect to increasing Φ may be explained in part by the fact that the stress-stretch curves for this material are rather flat at sufficiently large stretches (Fig. 3). As will be seen in Fig. 5, the *stretches* at which these instabilities occur in fact increase sharply with Φ. The maximum stress σ_m, as described at the end of Section 3, is also shown in this figure. For angle Φ less than $\simeq 27$ deg, bifurcation and loss of ellipticity occur before the maximum stress σ_m is reached while when Φ exceeds this value these phenomena occur after σ_m has been attained, i.e., at stretch ratios exceeding Λ_m.

In Fig. 5 we have plotted the logarithmic surface strains at instability, $\epsilon_b = ln\, \Lambda_b$ and $\epsilon_e = ln\, \Lambda_e$, under the preceding conditions. One observes again that for sufficiently small fiber angles Φ the fibers weaken the material against instability. As before, the distinction between σ_b and σ_e for Φ exceeding $\simeq 27$ deg is virtually impossible. Also not that the critical strains increase sharply with relatively small changes in the undeformed fiber angle Φ, and the predicted critical surface strain levels rapidly reach values that appear to be unrealistically high.

Figure 6 depicts the dependence of the bifurcation stress σ_b on the fiber angle Φ for the same material as before but in the case of compression ($\sigma < 0$).The stress at a loss of ellipticity in this case was considerably higher than σ_b and is thus not shown in this figure. (For example at $\Phi = 45$ deg it is found that $\sigma_e/\mu \simeq -19.5$.) We note two main differences between the tensile and compressive cases. In compression σ_b is highly dependent on the fiber angle Φ, presumably as a result of the steepness of the stress-stretch curves (Fig. 1). Secondly, bifurcation occurs at a stress level that is considerably smaller than σ_e. In contrast to the tensile case, here σ_b decrease with Φ. We also note that the reinforced material is weaker than

the unreinforced one for the fiber angles close to 90 deg (see also Arcisz [6]).

To investigate the effect of the material properties on stability, we have changed both the "fiber density" parameter α and the "fiber stiffness' parameter m and recalculated σ_b and σ_e in the case of tension. The variation of σ_e is shown in Fig. 7, with σ_b having values very close to σ_e as in the case discussed previously. It is of interest to note that the increase in m does not seem to significantly alter the stability properties of the material, for small angles Φ.

In conclusion, the results presented here for the particular Blatz-Ko material indicate that reinforcement in the direction of stressing provides the "greatest stability" in the case of tensile loading but "weakens" the material in the case of compression. The opposite is true when the fibers are normal to the load.

Acknowledgments

The results reported in this paper were obtained in the course of an investigation supported in part by the National Science Foundation through Grant CME 81-06581.

References

1 Blatz, P. J., and Ko, W. L., "Application of Finite Elastic Theory to the Deformation of Rubbery Materials," *Transaction of the Society of Rheology*, Vol. 6, 1962, pp. 223–251.

2 Knowles, J. W., and Sternberg, E., "On the Ellipticity of the Equations of Nonlinear Elastostatics for a Special Material," *Journal of Elasticity*, Vol. 5, 1975, pp. 341–361.

3 Biot, M. A., *Mechanics of Incremental Deformations*, Wiley, New York, 1965.

4 Hill, R., and Hutchinson, J. W., "Bifurcation Phenomena in the Plane Tension Test," *Journal of the Mechanics and Physics of Solids*, Vol. 23, 1975, pp. 239–264.

5 Kurashige, M., "Instability of a Transversely Isotropic Elastic Slab Subjected to Axial Loads," ASME JOURNAL OF APPLIED MECHANICS, Vol. 48, 1981, pp. 351–356.

6 Arcisz, M., "Bifurcation Conditions for Ideal Fiber-Reinforced Materials," *International Journal of Solids and Structures*, Vol. 16, 1980, pp. 1109–1121.

7 Rice, J. R., "The Localization of Plastic Deformation," *Proceedings of the 14th IUTAM Congress*, Koiter, W. T., ed., Delft, Netherlands, Aug. 1976, pp. 207–220.

8 Knowles, J. K., and Sternberg, E., "On the Failure of Ellipticity of the Equations for Finite Elastostatic Plane Strain," *Archive for Rational Mechanics and Analysis*, Vol. 63, 1977, pp. 321–326.

9 Douglas, W. J., and Jaunzemis, W., "Stability of Prestrained Laminated Media," *Proceedings of the 5th Symposium on Naval Structural Mechanics*, Wendt, F. W., et al., eds., 1967, pp. 679–700.

10 Spencer, A. J. M., *Deformations of Fiber-Reinforced Materials*, Oxford University Press , 1972.

11 Hutchinson, J. W., and Tvergaard, V., "Surface Instabilities on Statically Strained Plastic Solids," *International Journal of Mechanical Sciences*, Vol. 22, 1980, pp. 339–354.

12 Schwartz, L., *Theorie des Distributions*, Herrmann, 1950.